Journal of Sound and Vibration (1998) **218**(3), 405–418
Article No. sv981865

FORCE-STATE MAPPING METHOD OF A CHAOTIC DYNAMICAL SYSTEM

K. Shin and J. K. Hammond

ISVR, *University of Southampton*, *Highfield*, *Southampton SO*17 1*BJ*, *England*

(*Received* 23 *October* 1996, *and in final form* 2 *June* 1998)

This paper is concerned with the system identification of an experimental chaotic system. A conventional double-well potential vibrator is modified to accommodate an external air dash-pot damper. Damping can be controlled and set to have either high or low damping. The system exhibits very rich dynamics from periodic to chaotic states. The force-state mapping identification method is applied to both linear and chaotic states with the emphasis on quantifying the damping property for both high and low damping. This points to the potential use in condition monitoring of chaotic systems.

1. INTRODUCTION

Chaotic motion of the double-well potential vibrator have been extensively studied over the last couple of decades. For example, Moon and Holmes [1] studied motions of a thin steel beam buckled between two magnets, and established firm theoretical and experimental evidence of chaotic behaviour of this type of vibrator. However, not many articles can be found relating to system identification or identifying some physical parameters of the system. This paper is mainly focused on identifying system parameters with the emphasis on quantifying the damping property.

In general, system identification methods for dynamical systems may be classified into two groups: one is the parametric approach and the other non-parametric. Parametric methods seek to determine the values of parameters in an assumed model of the system to be identified, while non-parametric methods produce the best functional representation of the system without *a priori* assumptions about the system model. For system identification of non-linear systems, if all state variables, the acceleration signal and input signal are available together with knowledge of the mass, one can use the force-state mapping method. The 'force-state mapping' technique, which is a non-parametric method, was first introduced by Marsi and Caughey in 1979 [2]. Later in 1985, O'Donnell and Crawley independently developed a similar method and named it the 'force-state mapping' [3–7]. Since then, this technique has been applied to various engineering fields and developed further, especially by Worden and Tomlinson [8–10], Al-Hadid and Wright [11–15], and Lo [16]. The usefulness of this method is that

0022–460X/98/480405 + 14 $30.00/0

one can estimate (all) the system parameters. This method has been applied to various non-linear systems over the last couple of decades, but it has not been reported for chaotic systems. This paper demonstrates how well the force-state mapping technique can be applied to a practical chaotic system.

The beam studied in this paper is similar to the "Moon Beam" in reference [1] in principle, and its dynamics are very similar to the Duffing type oscillator. However, unlike the "Moon Beam", the shaker is used directly on the cantilever beam and a dash-pot air damper is also introduced to control the amount of damping in the system. The damper is set to produce two cases by adjusting the damper plug giving high and low damping. When the magnets are removed the beam becomes a simple linear cantilever beam. The force-state mapping method is applied to this experimental set-up to identify system parameters for both the linear system (without magnets) and the non-linear system (with magnets). The excitation signal in the case of the linear system is an amplitude modulated sinusoidal signal. For a non-linear system, the amplitude modulated sinusoidal signal may not be successful since the motion of the beam behaves in a complex way and does not cover the state space effectively when the input amplitude gets large. This is due to the magnets which attract the beam. However, when the beam is excited by a single sinusoidal signal with a certain amplitude level, its motion becomes chaotic. Although the input signal is a single sinusoid, because the motion is chaotic it covers a wide range of the state space. Thus it makes it possible to use the force-state mapping method. In this case, however, one must be very careful about the estimation of the "effective mass" which will be discussed later.

2. DESCRIPTION OF THE EXPERIMENTS AND MOTIONS OF THE BEAM

The mechanical system studied here is a cantilever beam buckled by two magnets as illustrated in Figure 1. This system is similar to the magneto-elastic oscillator of Moon and Holmes [1]. They used a very flexible thin steel beam clamped at one end, and the whole device was driven by a shaker. However, their beam was very thin (0·23 mm), so it was difficult to introduce an external damper. Thus, for the experiment in this paper, a device was constructed which can accommodate a dash-pot damper. A thin steel beam with dimensions 365 mm $\times$ 25 mm $\times$ 1 mm is clamped at the top of the experimental rig. At 70 mm from the free end of the beam, a dash-pot air damper is introduced. This damper can be controlled by adjusting the amount of air flow using a plug provided in the damper. Two magnets are secured on a steel plate near the free end of the beam to provide non-linear buckling forces. A sinusoidal signal from a signal generator is fed to an electromagnetic shaker through a power amplifier, with a signal being generated by a PC. The beam is then excited by an electromagnetic shaker at 60 mm from the clamped end of the beam. A force transducer is placed between the beam and the shaker, and a full bridge strain gauge is attached near the clamped end of the beam. The force and strain gauge signals are fed to an oscilloscope and a PC with a data acquisition system. Provided that the motion of the beam is dominated by one mode only, the strain gauge signal can be

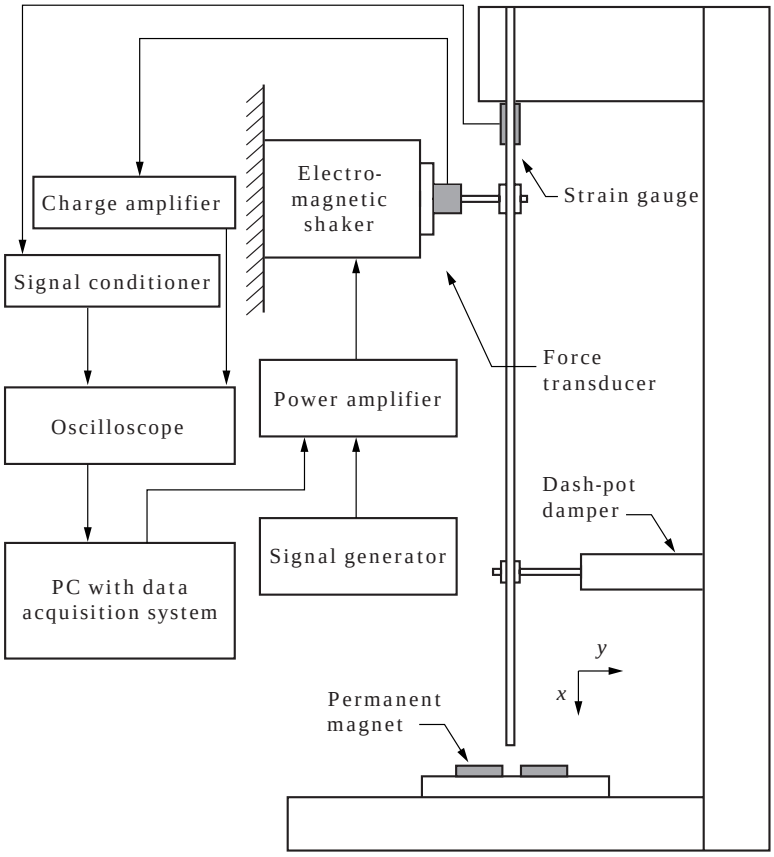

Figure 1. Experimental set-up.

transformed to a corresponding displacement signal, since the bending strain (ε_x) is proportional to the lateral displacement (y) such that

$$\varepsilon_x = ky. \tag{1}$$

The constant k is found by measuring the strain gauge bridge output for a given static displacement. For this experimental set-up, one can directly relate the beam tip displacement and the output of the signal conditioner (amplifier) of the bridge.

As described in references [1, 7], the equations of motion for a single degree of freedom approximation can be written as

$$m\ddot{q}(t) + c\dot{q}(t) - \alpha q(t) + \beta q^3(t) = A\cos(\omega t). \tag{2}$$

Equation (2) is in the form of a Duffing equation, and so the experimental set-up can be considered as a Duffing oscillator provided that the motion of the beam is dominated by the lowest mode only.

The Duffing oscillator is a single degree of freedom non-linear system with two stable equilibrium points and an unstable equilibrium point. Chaotic motion from a Duffing oscillator is generated when the motion evolves around the two magnets almost irregularly. In the experimental set-up, two stable equilibrium points are

the centre of each magnet, and the unstable equilibrium point is between the two magnets. To make sure that the beam behaves like a single degree of freedom system, the motion of the beam should be dominated by its lowest mode during the experiment. Assuming that the excitation frequency is near the first natural frequency of the linear system (without magnets) results in the motion of the beam being dominated by the lowest mode. A sinusoidal signal with a single frequency is chosen to insure this. The natural frequencies of the beam without magnets (i.e., in linear state) were measured, and the lowest natural frequency is about 7·1 Hz. The effect of the introduction of the magnets is to increase stiffness and introduce non-linearity, but for low amplitude motion the 'natural frequency' is shifted upwards slightly. During the experiment, the beam is excited at 7 Hz, and it is observed that this results in the motion of the beam being dominated by the first mode.

It is now briefly demonstrated how the experimental system changes from periodic motion to chaotic motion by presenting both time series and pseudo phase space (reconstructed phase portrait using the 'method of delays') [18] for each case of different motions. Starting with a small amplitude for the input signal, the motions of the beam are examined by gradually increasing the amplitude of the input signal with a fixed frequency (7 Hz). When the amplitude of the input signal is small, the beam oscillates around one of the equilibrium points. The fundamental period of the motion is the same as the period of the input signal, i.e., period-1 motion as shown in Figure 2(a) and (b). As the amplitude increases the motion becomes period-2, period-3, etc., and finally it becomes chaotic. These are shown in Figure 2. Note that these are experimental results. It is also found experimentally that the motion after period-3 is very sensitive to the amplitude applied, so a small increase of amplitude causes chaotic motion. Thus, it is very difficult to observe the higher order subharmonic motions beyond period-3. This may be due to the finite precision of the experimental devices which cannot control the input amplitude precisely. However, from Figure 2, one can see that chaotic motion arises after subharmonic motion.

It has been shown how the experimental set-up behaves like the Duffing equation in a specific case, and several types of motion of the beam, depending on the amplitude of excitations, have been presented. In the following section, system parameters in (2) are obtained from the force-state mapping technique, and a comparison is made between linear and non-linear systems.

3. SYSTEM IDENTIFICATION USING THE FORCE-STATE MAPPING METHOD

Consider the equation of motion of the SDOF system

$$m\ddot{x} + f(x, \dot{x}) = F(t) \tag{3}$$

where $f(x, \dot{x})$ is a function which denotes the restoring force of the system. Rearranging (3) gives

$$f(x, \dot{x}) = F(t) - m\ddot{x} = F_{net}. \tag{4}$$

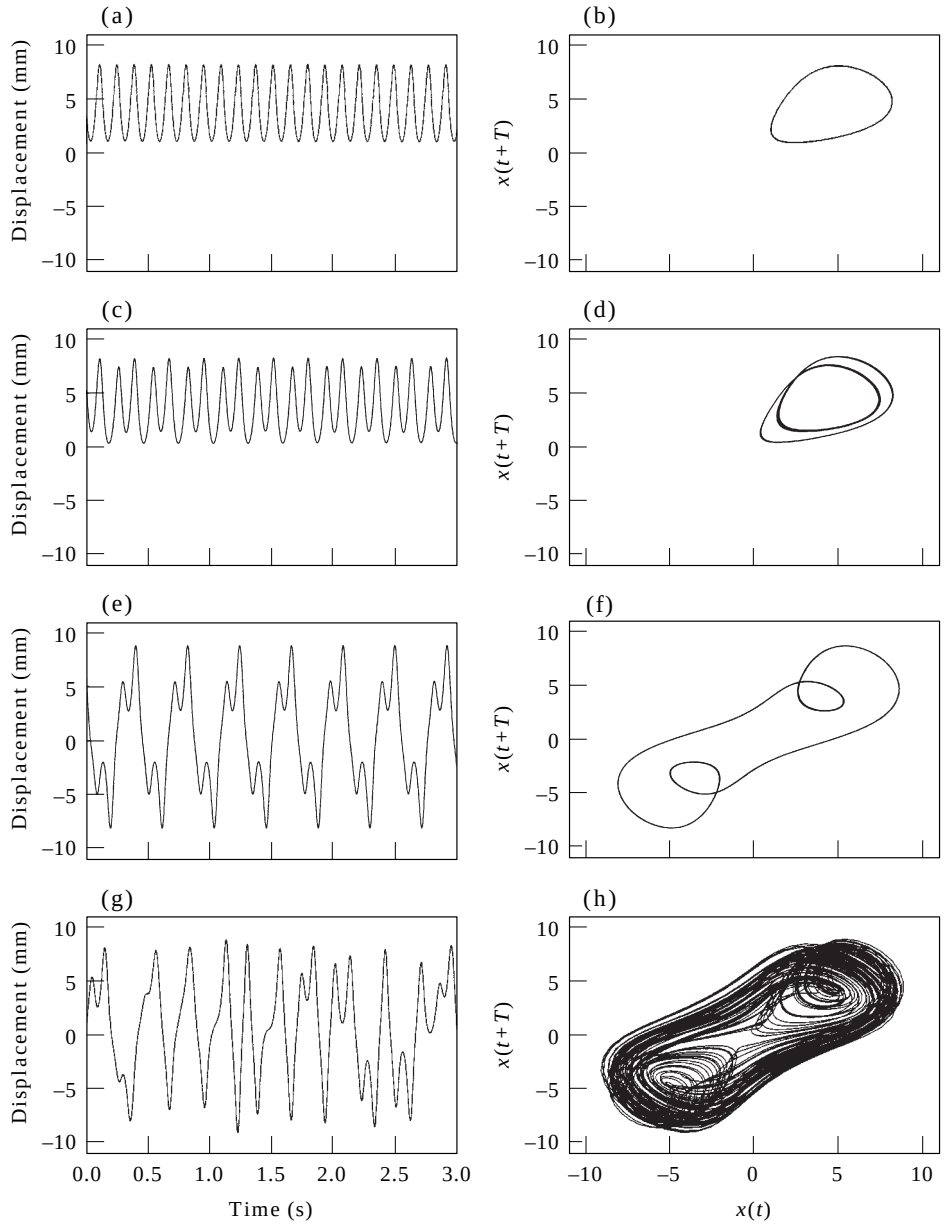

Figure 2. Different types of motions of the beam (forcing frequency 7 Hz). Pseudo phase portraits are constructed by the method of delays with delay time $T = 0{\cdot}026$ s. $x(t)$ denotes the displacement. (a) Time series of the period-1 motion. (b) Pseudo phase portrait of period-1 motion. (c) Time series of the period-2 motion. (d) Pseudo phase portrait of period-2 motion. (e) Time series of the period-3 motion. (f) Pseudo phase portrait of period-3 motion. (g) Time series of the chaotic motion. (h) Pseudo phase portrait of chaotic motion.

If the applied force, mass, and acceleration signal are known then one can construct a 3-dimensional plot of F_{net} versus x and $\dot{x}$. The state variables (x and $\dot{x}$) can be usually found by direct measurements or through integration of $\ddot{x}$. If the net force (F_{net}) is only a function of the state variables, then the 3-dimensional

plot produces a unique surface and the surface will be independent of the time history of the applied force. Therefore, any type of applied force can be used. However, the ability to produce a complete 'force-state map' requires that the force input signal excites the displacement (x) and velocity ($\dot{x}$) which adequately 'cover' the state space in such a way that the measurements are reasonably dense within the space. If there is a region in the state space which is not excited by the applied force, then there will be a 'hole' in the surface of the force-state map. Thus, the commonly used input force signals are random signals and modulated sinusoidal signals. Once the necessary signals (F_{net}, x and $\dot{x}$) have been obtained, the state signals are divided into 'grids' with designated 'representative points'. A representative point can be obtained by averaging all the F_{net} values whose corresponding state (x and $\dot{x}$) fall into the pre-determined specific grid [16]. This results in x being a row $\times$ 1 vector, $\dot{x}$ being a col $\times$ 1 vector, and F_{net} being a row $\times$ col matrix, where 'row' and 'col' are the number of grids for each signal. When this process is done, the state parameters can be obtained by curve fitting to the surface (e.g., Chebyshev polynomials by Marsi *et al*. [2]). In this paper, ordinary polynomials are used for the curve fitting, and the force-state mapping method is applied to both experimental linear systems and chaotic systems. In order to successfully apply the force-state mapping method, there are many things to be carefully considered. Any phase mismatches of devices will degrade the quality of the surface and should be avoided. For example, the charge amplifier used in this experiment had a 180° phase shift which had to be accounted for, and different devices have different phase delays associated with them. These characteristics must be carefully considered and accounted for. In general, it may be difficult to measure all the necessary signals simultaneously, so one usually measures acceleration and then obtains displacement and velocity signals by either time domain integration or frequency domain integration. However during chaotic motion in this experiment, which results in swinging from one equilibrium point to another, this produces large negative and positive offsets in measurements, making it difficult to use integration methods, since offset introduces a drifting effect. Thus, numerical differentiation is used after measuring the displacement signal which is obtained via the strain gauge bridge output. If $x(n)$ is the measured

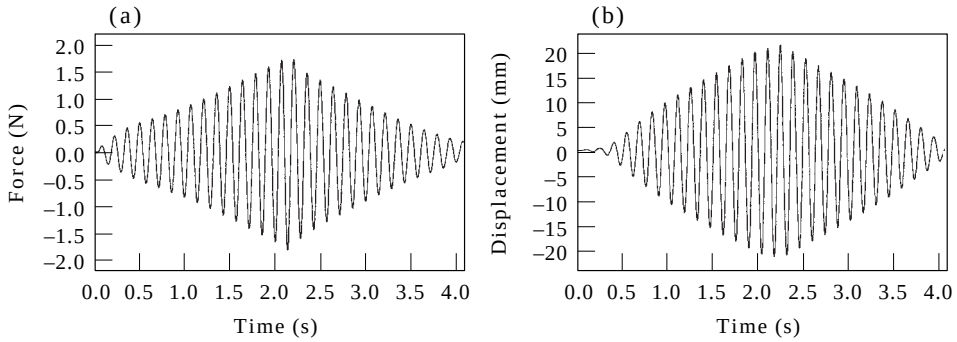

Figure 3. Input, output signal used for a linear system identification (forcing frequency 7 Hz). (a) Actual input force signal measured from a force transducer. (b) Measured displacement signal converted from the strain gauge bridge output.

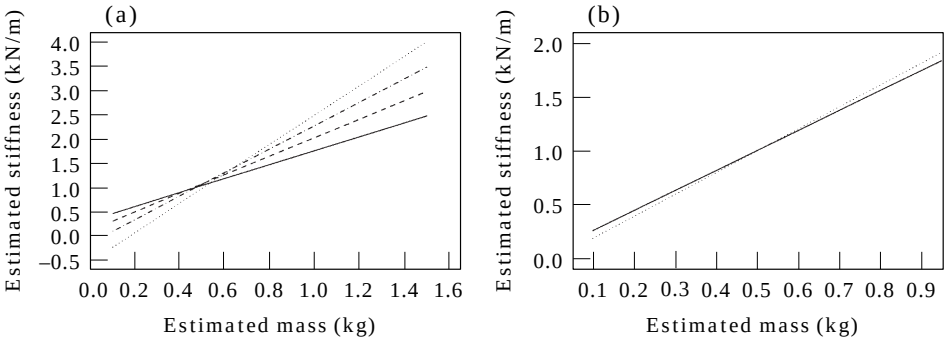

Figure 4. Mass estimation plot for a linear system using the sensitivity approach. (a) Estimated mass is varying from 0·42 to 0·65 kg (forcing frequencies: 6, 7, 8 and 9 Hz from solid line to dotted line). (b) Estimated mass is 0·52 kg (forcing frequency: 6·8 Hz for solid line and 7·2 Hz for dotted line).

discrete displacement time series with sampling rate $1/T$, then the velocity signal is obtained by using the central difference approximation [19], i.e.,

$$x'(n) = \frac{x(n-2) - 8x(n-1) + 8x(n+1) - x(n+2)}{12T}. \tag{5}$$

One drawback of numerical differentiation is noise on the measured signal. An 'insignificant' noise in the displacement signal may cause a very noisy acceleration for high frequency components. This problem can be alleviated by using the 'Iterative SVD method' which was developed by Shin [17]. It was shown that if the sampling rate is very high compared to the forcing frequency, then one can almost blindly use this method. Examples of noise reduction are shown together with the experimental results for linear systems. A particular problem is the estimation of mass, which is also discussed.

3.1. LINEAR SYSTEMS

If the two permanent magnets are not introduced and excitation is not too large, the experimental set-up becomes a simple linear cantilever beam. So the equation of motion for one mode (9) can be simply written as

$$c\dot{q}(t) + kq(t) = F(t) - m_e\ddot{q}(t) = F_{net}. \tag{6}$$

The system parameters c and k are now estimated by using the force-state mapping method. The input forcing signal is generated in the PC and then, through the DAC (Digital-Analogue Converter) and amplifier, it is fed to the shaker. The input signal used here is an amplitude modulated signal as shown in Figure 3.

Even in a simple linear system, correct estimation of the effective mass m_e is critical and has been studied extensively by a number of authors. If the geometry is simple like a cantilever beam, the effective mass (modal mass of the first mode) can be obtained directly by

$$m_e = \int_0^L m\phi^{\,2}\mathrm{d}x = \left(\frac{m}{\beta_1}\right)\int_0^{\beta_1 L}\phi^{\,2}\mathrm{d}\beta_1 x = \frac{3{\cdot}48\ \mathrm{m}}{\beta_1} \tag{7}$$

where, m is mass per unit length of the beam, and $\beta_1 L = 1{\cdot}8751$. The mass estimated by (7) for the experimental set-up is $m_e \approx 0{\cdot}13$ kg. However, for this estimated mass, the effects of additional masses are not included, i.e., dymamic mass of the shaker and the mass of the force transducer introduce additional mass. Because the cantilever beam is very light, the additional masses must be considered. Thus, the sensitivity approach method developed by Al-Hadid *et al*. [12–14] is used. Reference [14] briefly summarises the basic idea of this approach. Given a single degree of freedom system of the form of equation (3), if an incorrect mass $\hat{m}$ (assumed mass) is used then the incorrect restoring force $\hat{f}(x, \dot{x})$ is estimated. If the system is linear, then $\hat{f}(x, \dot{x}) = \hat{c}\dot{x} + \hat{k}x$, where $\hat{c}$ is the estimated damping and $\hat{k}$ is the estimated stiffness. For a linear system and a single sinusoidal

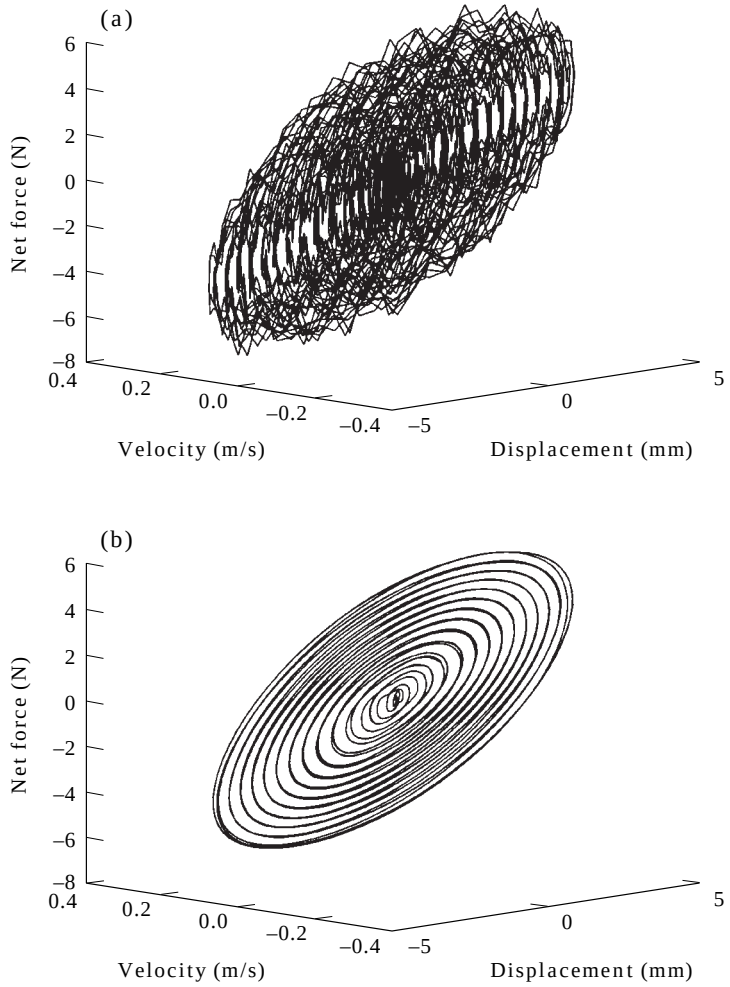

Figure 5. (a) Force-state plot of a linear system without the noise reduction technique (high damping). (b) Force-state plot of a linear system with the noise reduction technique (high damping).

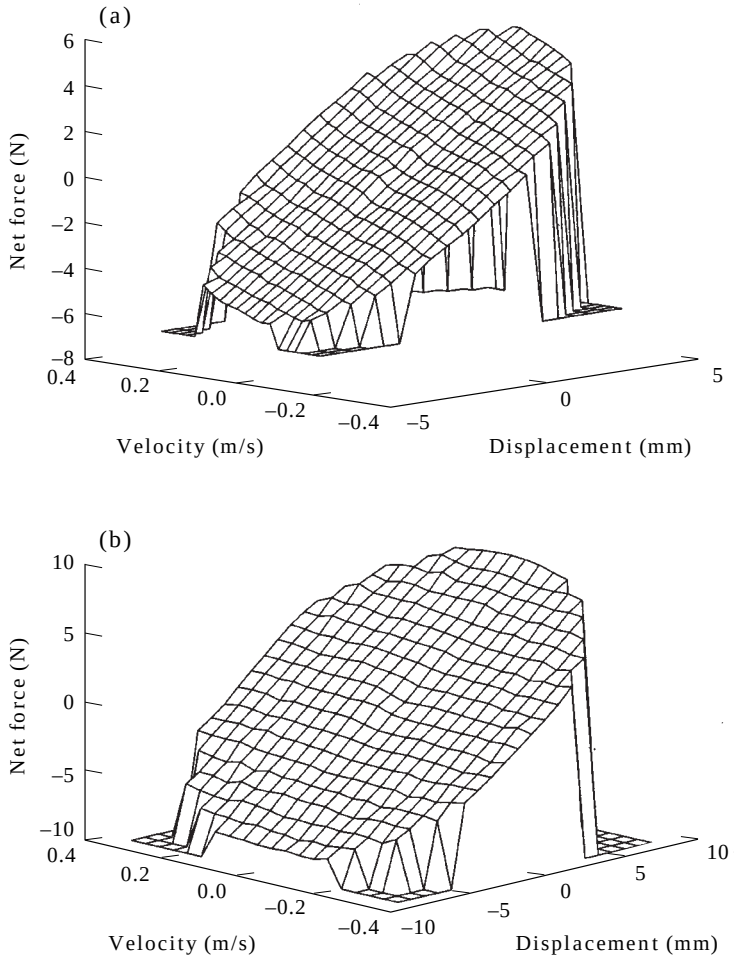

Figure 6. (a) Surface representation of the force-state map of a linear system (high damping). Estimated values of parameters: $c = 7{\cdot}3$ N · s/m and $k = 1{\cdot}008$ kN/m. (b) Surface representation of the force-state map of a linear system (low damping). Estimated values of parameters: $c = 2{\cdot}7$ N · s/m and $k = 1{\cdot}007$ kN/m.

frequency excitation (ω), the relationship between the estimated mass and the estimated stiffness is given by reference [14]

$$\hat{k} = (k - \omega^2 m) + \omega^2 \hat{m} \tag{8}$$

where, m and k are exact mass and stiffness respectively. Thus it is shown that the relationship between $\hat{m}$ and $\hat{k}$ is linear. Thus one can find the intersection point by plotting lines (estimated stiffness versus assumed mass) found from curve fits to measurements taken at two or more different excitation frequencies, assuming two initial mass values. In general, the system parameter for the plot is the stiffness term, but any system parameters can be used. If the system is a single degree of freedom system, any lines must intersect at one point. This relationship is also true for non-linear systems but depends on excitation amplitude [14]. However for a

continuous system like the thin cantilever beam used in this experiment, although the excitation frequencies are very near the first resonance frequency, the lines do not intersect at one point but vary from frequency to frequency as shown in Figure 4(a). This may be caused by the interference of higher modes. If this is true, the effective mass is different at each driving frequency although the overall behaviour of the system is like a single degree of freedom system. However, the effective masses at neighbouring frequencies should not differ greatly from each other. Thus, in this experiment, the driving frequency is decided and then the sensitivity approach is performed using frequencies very near the driving frequency. The driving frequency is chosen at 7 Hz which is very close to the first natural frequency of the beam, and the frequencies at 6·8 and 7·2 Hz used for the sensitivity approach. This is shown in Figure 4(b), and the estimated effective mass is 0·52 kg. This method is carried out in exactly the same way for the non-linear systems described in section 3.2.

Once the correct effective mass is estimated, one can now produce the surface representation of the system. However, noise introduced through the numerical differentiation cannot be ignored. A 3-dimensional plot of net force versus state variables without any noise reduction technique is shown in Figure 5(a). Using the 'Iterative SVD method', this noise can be significantly reduced as shown in Figure 5(b). The details of this noise reduction technique can be found in reference [17]. The 3-dimensional surface representation is shown in Figure 6(a) for the highly damped system, and in Figure 6(b) for the case of the weakly damped system. From Figure 6, the estimated values of the parameters by polynomial curve fitting are $c = 7{\cdot}3$ N · s/m and $k = 1{\cdot}008$ kN/m for the case of high damping, and $c = 2{\cdot}7$ N · s/m and $k = 1{\cdot}007$ kN/m for the case of low damping. The results are promising since the change of the property of air dash-pot damper (which is

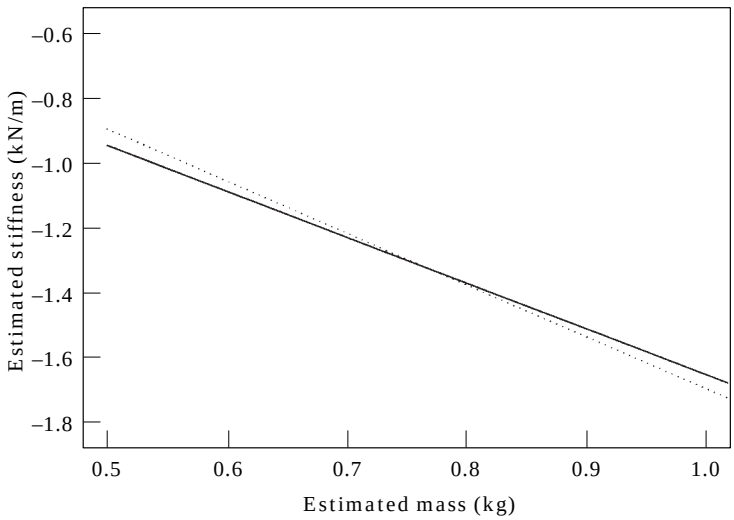

Figure 7. Mass estimation plot for a chaotic system using the sensitivity approach. Estimated mass is 0·77 kg (forcing frequency: 6·8 Hz for solid line and 7·2 Hz for dotted line).

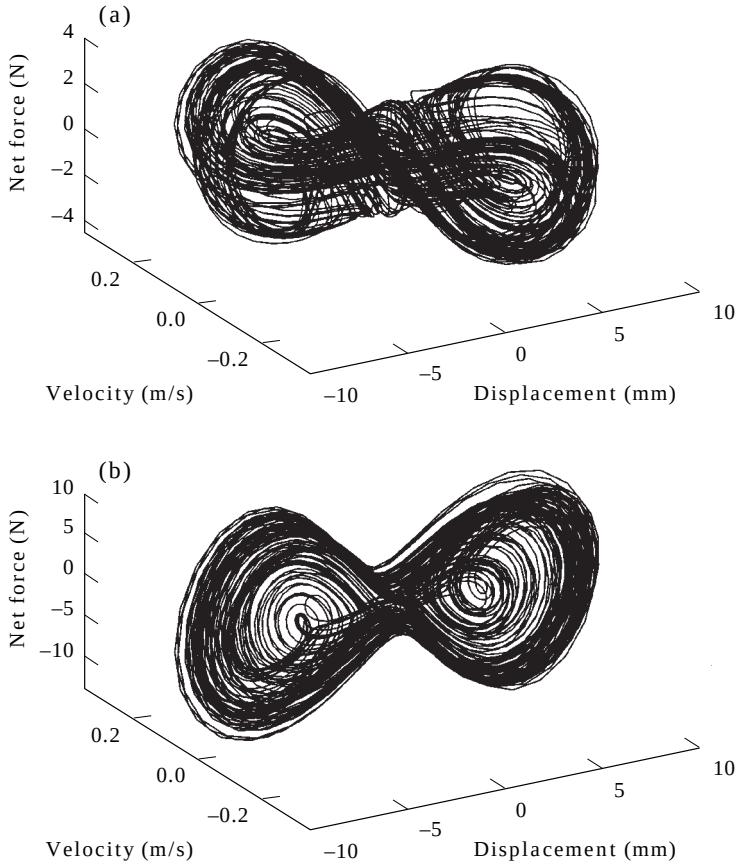

Figure 8. (a) Bad choice of the assumed mass. Force-state plot of a chaotic system with an assumed mass 0·2 kg (low damping). (b) Right choice of the assumed mass. Force-state plot of a chaotic system with an assumed mass 0·7 kg (low damping).

assumed to be linear) causes only a change of the damping coefficient while the stiffness term remains almost the same.

3.2. NON-LINEAR (CHAOTIC) SYSTEM

The equation of motion (2) can be rearranged as

$$c\dot{q}(t) - \alpha q(t) + \beta q^3(t) = F(t) - m_e\ddot{q}(t) = F_{net}. \tag{9}$$

For the forcing signal $F(t)$, one may attempt to use the same signal as in the case of the linear system. However, it was found that the short duration of the amplitude modulated signal fails to excite a large area of the state space. The motion of the beam becomes chaotic as soon as the amplitude gets large, producing a 'hole' in the state space. However, if the beam is excited with a single sinusoidal signal in a chaotic regime over a long time, the motion is chaotic and a large area of state space will be covered. Thus the forcing signal for this case is chosen as a sinusoidal signal creating a chaotic regime.

The effective mass estimation is carried out in the same way as described in section 3.1. As shown in Figure 7, the effective mass is estimated as 0·77 kg. For linear systems, any assumed masses can be used to estimate the effective mass of the system. However, one must be careful when the sensitivity approach is used for a chaotic system. Unlike the linear system, the 3-dimensional plot of net force versus state space using a significantly different mass from the true effective mass will result in almost no structure. This makes it impossible to estimate the effective mass, since the estimated system parameters corresponding to the assumed mass is obtained from the estimated force-state surface constructed by using the assumed mass. An example of a bad choice of assumed mass is shown in Figure 8(a) with an assumed mass 0·2 kg, and Figure 8(b) shows the example of right choice of the assumed mass (0·7 kg). Thus assumed mass must be chosen carefully. We simply use the sensitivity approach on a trial and error basis, i.e., one can construct the 3-dimensional plot using from a very small assumed mass

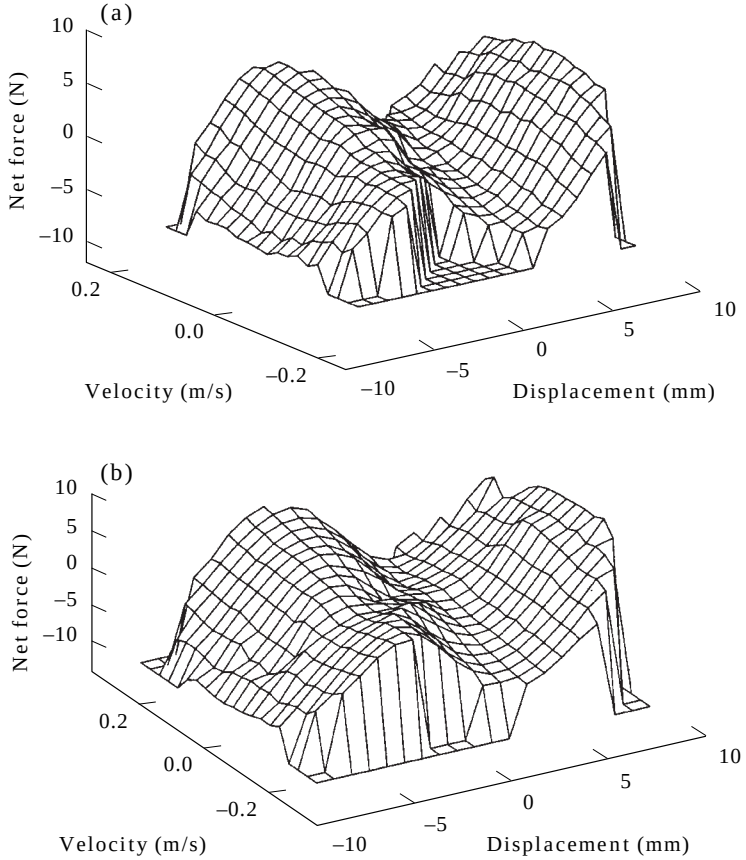

Figure 9. (a) Surface representation of the force-state map of a chaotic system (high damping). Estimated values of parameters: $c = 8{\cdot}6$ N · s/m, $\alpha = -1{\cdot}3$ kN/m, and $\beta = 56{\cdot}1$ MN/m^3. (b) Surface representation of the force-state map of a chaotic system (low damping). Estimated values of parameters: $c = 3{\cdot}0$ N · s/m, $\alpha = -1{\cdot}4$ kN/m, and $\beta = 54{\cdot}9$ MN/m^3.

TABLE 1

Summary of the experimental results

Cases	c (N · s/m)	k (kN/m)	α (kN/m)	β (MN/m^3)
Linear (low damping)	$2{\cdot}7 \pm 0{\cdot}8$	$1{\cdot}0 \pm 0{\cdot}1$		
Linear (high damping)	$7{\cdot}3 \pm 0{\cdot}6$	$1{\cdot}0 \pm 0{\cdot}1$		
Chaos (low damping)	$3{\cdot}0 \pm 1{\cdot}2$		$1{\cdot}4 \pm 0{\cdot}2$	$54{\cdot}9 \pm 0{\cdot}6$
Chaos (high damping)	$8{\cdot}6 \pm 1{\cdot}2$		$1{\cdot}3 \pm 0{\cdot}1$	$56{\cdot}1 \pm 0{\cdot}6$

to a very large assumed mass by incrementing the assumed mass, and finding the region where the structure is revealed.

Using the estimated effective mass, the surface representation of the system is produced. The surface representation is shown in Figure 9(a) for the high damping system, and in Figure 9(b) for the case of low damping. From these figures, the estimated values of the parameters by polynomial curve fitting are $c = 8{\cdot}6$ N · s/m, $\alpha = 1{\cdot}3$ kN/m, and $\beta = 56{\cdot}1$ MN/m^3 for the case of high damping, and $c = 3{\cdot}0$ N · s/m, $\alpha = 1{\cdot}4$ kN/m, and $\beta = 54{\cdot}9$ MN/m^3 for the case of low damping. The results are almost the same as the case of linear systems, i.e., only an increase of damping coefficient while the other parameters remain almost the same, but the damping coefficient of the chaotic system should not differ from that of the corresponding linear system. However, there is a small difference between the linear system and chaotic system in the estimation of the damping parameter. In spite of this small difference, considering many aspects of measurements and numerical procedures, one can consider the difference is insignificant, and the results can be considered as satisfactory.

4. DISCUSSION

In this paper, the force-state mapping method has been successfully applied to a practical experimental set-up. To the author's knowledge, it is the first time that the force-state mapping method has been successfully applied to a chaotic system. The results of both linear and non-linear systems are compared by changing the condition of damping while the other parameters remain the same. These are summarised in Table 1, and are obtained using four segments of the experimental data. From this, it is shown that there is good agreement between the two systems, i.e., the estimated damping parameters of both linear and non-linear systems are very similar while the other parameters are unchanged for both high and low damping. The results presented in this paper are very promising, and so may be further investigated in condition monitoring of chaotic systems.

REFERENCES

1. F. C. MOON and P. J. HOLMES 1979 *Journal of Sound and Vibration* **65**, 275–296. A magnetic strange attractor.

2. S. F. Marsi and T. K. Caughey 1979 *Transactions of the ASME*: *Journal of Applied Mechanics* **46**, 433–447. A nonparametric identification technique for nonlinear dynamic problems.
3. K. J. O'Donnell and E. F. Crawley 1985 Space Systems Laboratory, Massachusetts Institute of Technology, Cambridge, Rept. #16–85. Identification of non-linear parameters in space structure joints using force-state mapping technique.
4. E. F. Crawley and A. C. Aubert 1986 *American Institute of Aeronautics and Astronautics Journal* **24**, 155–162. Identification of nonlinear structural elements by force-state mapping.
5. E. F. Crawley and K. J. O'Donnell 1986 *Collection of Technical Papers—AIAA/ASME/ASCE/AHS Structures*, *Structural Dynamics & Materials* 27*th Conference* **1**, 659–667. Identification of nonlinear system parameters in joints using the force-state mapping technique.
6. E. F. Crawley and K. J. O'Donnell 1986 *Proceedings of the* 10*th U.S. National Congress of Applied Mechanics*, 415–420. Incorporation of the effects of material damping and nonlinearities on the dynamics of space structures.
7. E. F. Crawley and K. J. O'Donnell 1987 *American Institute of Aeronautics and Astronautics Journal* **25**, 1003–1010. Force-State mapping identification of nonlinear joints.
8. K. Worden and G. R. Tomlinson 1988 *Proceedings of the* 6*th International Modal Analysis Conference* **2**, 1471–1479. Developments in force state mapping for nonlinear systems.
9. K. Worden and G. R. Tomlinson 1989 Proceedings of the 7th International Modal Analysis Conference **2**, 1347–1355. Application of the restoring force surface method to nonlinear elements.
10. C. Surace, K. Worden and G. R. Tomlinson 1992 *Technical Paper*, *Proceedings of the Institution of Mechanical Engineers*. *Part D*, *Journal of Automobile Engineering* **206**. On the non-linear characteristics of automotive shock absorbers.
11. M. A. Al-Hadid and J. R. Wright 1989 *Mechanical Systems and Signal Processing* **3**, 269–290. Developments in the force-state mapping technique for non-linear systems and the extension to the location of non-linear elements in a lumped-parameter system.
12. M. A. Al-Hadid and J. R. Wright 1990 *Mechanical Systems and Signal Processing* **4**, 463–482. Application of the force-state mapping approach to the identification of non-linear systems.
13. J. R. Wright and M. A. Al-Hadid 1991 *The International Journal of Analytical and Experimental Modal Analysis* **6**, 89–103. Sensitivity of the force-state mapping approach to measurement errors.
14. M. A. Al-Hadid and J. R. Wright 1991 *Structural Dynamics*: *Recent Advances*, *Proceedings of the* 5*th International Conference*, 399–410. A method for the estimation of mass and modal mass in the identification of nonlinear single and multi degree of freedom systems using the force-state mapping approach.
15. M. A. Al-Hadid and J. R. Wright 1992 *Mechanical Systems and Signal Processing* **6**, 381–401. Estimation of mass and modal mass in the identification of nonlinear single and multi degree of freedom systems using the force-state mapping approach.
16. H. R. Lo 1988 *Ph.D. thesis*, *University of Southampton*. System characterisation and identification of non-linear systems (with particular reference to hysteretic systems).
17. K. Shin 1996 *Ph.D. thesis*, *University of Southampton*. Characterisation and identification of chaotic dynamical systems.
18. F. Takens 1980 *Lecture Notes in Mathematics* **898**, 365–381. Detecting strange attractors in turbulence.
19. J. Penny and G. Linfield 1995 *Numerical Methods using Matlab*. Chichester: Ellis Horwood.